HHS Public Access

Author manuscript

Anal Chem. Author manuscript; available in PMC 2018 April 07.

Published in final edited form as:

Anal Chem. 2016 October 18; 88(20): 10143–10150. doi:10.1021/acs.analchem.6b02678.

Greatly Increasing Trapped Ion Populations for Mobility Separations Using Traveling Waves in Structures for Lossless Ion Manipulations

Liulin Deng, **Yehia M. Ibrahim**, **Sandilya V. B. Garimella**, **Ian K. Webb**, **Ahmed M. Hamid**, **Randolph V. Norheim**, **Spencer A. Prost**, **Jeremy A. Sandoval**, **Erin S. Baker**, and **Richard D. Smith***

Biological Sciences Division and Environmental Molecular Sciences Laboratory, Pacific Northwest National Laboratory, Richland, Washington 99352, United States

Abstract

The initial use of traveling waves (TW) for ion mobility (IM) separations using structures for lossless ion manipulations (SLIM) employed an ion funnel trap (IFT) to accumulate ions from a continuous electrospray ionization source and was limited to injected ion populations of ~10^6 charges due to the onset of space charge effects in the trapping region. Additional limitations arise due to the loss of resolution for the injection of ions over longer periods, such as in extended pulses. In this work a new SLIM “flat funnel” (FF) module has been developed and demonstrated to enable the accumulation of much larger ion populations and their injection for IM separations. Ion current measurements indicate a capacity of ~3.2×10^8 charges for the extended trapping volume, over an order of magnitude greater than that of the IFT. The orthogonal ion injection into a funnel shaped separation region can greatly reduce space charge effects during the initial IM separation stage, and the gradually reduced width of the path allows the ion packet to be increasingly compressed in the lateral dimension as the separation progresses, allowing efficient transmission through conductance limits or compatibility with subsequent ion manipulations. This work examined the TW, rf, and dc confining field SLIM parameters involved in ion accumulation, injection, transmission, and IM separation in the FF module using both direct ion current and MS measurements. Wide m/z range ion transmission is demonstrated, along with significant increases in the signal-to-noise ratios (S/N) due to the larger ion populations injected. Additionally, we observed a reduction in the chemical background, which was attributed to more efficient desolvation of solvent related clusters over the extended ion accumulation periods. The TW SLIM FF IM module is anticipated to be especially effective as a front end for long path SLIM IM separation modules.

Graphical abstract

*Corresponding Author. Phone: 509-371-6219. Fax: 509-371-6564. rds@pnnl.gov.

ASSOCIATED CONTENT

Supporting Information

The Supporting Information is available free of charge on the ACS Publications website at DOI: 10.1021/acs.analchem.6b02678.

Space charge effects on ion accumulation (PDF)

The authors declare no competing financial interest.

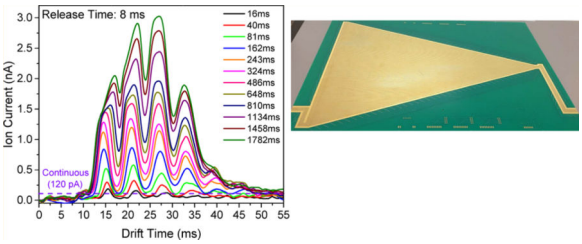

Electrospray ionization (ESI)[1] coupled with ion mobility-mass spectrometry (IM-MS)[2] is an increasingly utilized and potentially powerful approach with broad applications in metabolomics,[3–6] glycomics,[7] proteomics, etc.[8–12] Increases in the resolution, sensitivity, and dynamic range of IM-MS measurements are important for the analysis of complex samples.[13–16] The size of an ion population injected for IM separation is a key consideration, ultimately setting limits to the sensitivity and dynamic range and impacting essentially every aspect of platform performance, including ion utilization efficiency. For example, ions from electrospray ionization (ESI) are typically continuously generated, but conventional drift tube IM separations are discontinuous, requiring injection of a tightly bunched ion packet, and usually only a very small fraction of generated ions are utilized.[17] Multiplexing techniques, such as Fourier,[17,18] Hadamard,[19,20] and phase-resolved ion gating,[21] have been employed to improve the IM duty cycle and enhance the overall ion utilization efficiency, but suffer limitations for many applications, for instance, mass spectral “deconvolution” is generally imperfect, and the ability to isolate low-abundance species for MS/MS analysis is greatly reduced.

We have previously developed an electrodynamic ion funnel trap (IFT)[22,23] to provide an increased trapping volume for external ion accumulation prior to injection for IM-MS. The IFT significantly increased the overall ion utilization efficiency, providing an order of magnitude improvement in sensitivity with IM separations.[24] Other ion storage geometries have also been used for ion accumulation and to improve the duty cycle.[25,26] An rf ion guide incorporating a trapping gate has been similarly used to accumulate ions for traveling wave (TW) IM-MS[27,28] Regardless of the platform details, the sensitivity for pulsed introduction of ions for IM-MS ultimately becomes limited by the trap space charge capacity. Space charge effects serve to provide limitations for both quantitative unbiased ion accumulation as well as the maximum capacity.[29–31]

Recently, structures for lossless ion manipulations (SLIM) have been developed and initially demonstrated for a range of ion manipulations, including IM separations, ion trapping, and ion switching between different ion paths.[32–35] Compact “straight” and “multiturn”[36,37] TW-based SLIM modules have also been developed and characterized and achieved IM separations comparable to somewhat longer (~1 m) drift tube (DT) designs. The TW SLIM IM modules were fabricated using printed circuit board (PCB) technology and provided benefits of simpler design compared to previous drift SLIM IM modules, most significantly the elimination of the need for progressively higher dc voltages as path length increases. Such TW SLIM designs are not only attractive for providing a route to achieving greater IM resolution but also offer a simple route for enabling more complex sequences of ion reactions, ion selection, or extended storage based upon the ability to fabricate modules

allowing complex manipulations that can function in an essentially lossless fashion. Recently we reported on a 13-m long serpentine path TW SLIM module and initially demonstrated high efficiency ion transmission in conjunction with much higher IM resolution separations for a range of samples.[38,39] This work provides a foundation for achieving ultrahigh IM resolution using either longer path or multipass designs, or the possibility of a combination of both, for improved analyses of complex mixtures with the ability to distinguish, e.g., biologically relevant isomers that are presently intractable.

However, to this point our SLIM IM modules have used an external IFT identical to that employed with our drift tube IMMS to accumulate and inject ions. The maximum charge capacity of IFT has been previously determined to be ~3×10^7 charges, with a more useful charge capacity of ~6×10^6 when space charge effects that introduce biases in the accumulation process are to be avoided.[24] Because of the greater separation times in a long serpentine path TW SLIM IM, the overall ion utilization efficiency from a continuous ESI source using the IFT is estimated to be <1%.[39] Additionally, in such extended IM separations the broadening of IM peaks will significantly limit possible improvements in the characterization of complex mixtures unless injected ion populations can be increased. Finally, a larger ion trap capacity makes more effective use of ions produced from small samples and provides a basis for optimizing the analytical information obtainable.

In order to improve the ion utilization efficiency, sensitivity, and overall effectiveness of the TW SLIM IM modules, we have developed and characterized a TW SLIM FF module that enables ion accumulation, trapping, and injection in conjunction with more than a 10-fold increase in both the maximum and quantitatively useful charge capacities. The FF significantly enhances the ion utilization efficiency and is shown to provide an ~10-fold increase in IM-MS sensitivity compared to the IFT.[24] In addition, we have observed the extended accumulation and trapping to provide a significant reduction in the MS “chemical” background.

EXPERIMENTAL SECTION

Mass Spectrometry

Ions were generated by a nanoelectrospray ionization (nano-ESI) source (3000 V) using a chemically etched emitter (20-μm i.d.) connected to a 30-μm i.d. fused-silica capillary (Polymicro Technologies, Phoenix, AZ) through a zero volume stainless steel union (Valco Instrument Co. Inc., Houston, TX). Sample solutions were infused at a flow rate of 0.3 μL/min. Ions were introduced into the first stage of vacuum through a heated (130 °C) 500-μm i.d. stainless steel capillary (Figure 1A). After exiting the capillary, ions were transported through an ion funnel trap (IFT, 950 kHz and ~200 V_{pp}) at 2.95 Torr (the IFT was used in a continuous mode in this work; i.e., without trapping).[24] The inlet capillary was offset from the center axis of the IFT by 6 mm to minimize the transmission of neutral particles through the IFT and conductance-limiting orifice as well as to effectively eliminate gas dynamic effects in the SLIM chamber. Upon exiting the IFT, ions passed through a conductance-limiting orifice (2.5 mm i.d.) into the TW SLIM FF module (3 Torr nitrogen). The differential positive pressure of 50 mTorr further prevents neutrals from entering the TW SLIM FF module. The SLIM chamber was supplied with high-purity nitrogen filtered

through hydrocarbon and moisture traps. After drifting through the TW SLIM FF module, a 15 cm long “rear” ion funnel (RIF) (820 kHz and ~120 V_{pp}) with a 23 V/cm dc gradient was used to focus ions through a conductance limiting orifice (2.5 mm i.d.) into the differentially pumped region (0.46 Torr) containing a short rf-only quadrupole (1 MHz and ~130 V_{pp}). The quadrupole was used also to measure transmitted ion currents from the TW SLIM FF module in this work. Ions were then transmitted into an Agilent 6224 TOF MS equipped with a 1.5-m flight tube (Agilent Technologies, Santa Clara, CA). Data were acquired using a U1084A 8-bit ADC digitizer (Keysight Technologies, Santa Rosa, CA) and processed using in-house control software written in C#.

TW SLIM Flat Funnel Module

The TW SLIM FF module consisted of a pair of parallel PCBs (45.9 cm long × 32.5 cm wide) spaced by a gap of 3.15 mm. Figure 1B depicts the intersection region of one of the surfaces (the opposing surface has a mirror image electrode design) showing the electrode arrangements of rf, TW, and guard electrodes in different sections as well as the dual gate (G1 and G2) electrodes. All rf electrodes are interleaved with TW electrodes extending throughout the TW SLIM FF module where out-of-phase rf waveforms are applied to adjacent rf electrodes to confine ions orthogonally to the electrode surfaces. The rf creates a pseudopotential that prevents ions from being lost to the electrode surfaces. All rf strip electrodes are 0.43 mm wide, the TW electrodes are 1.03 mm long and 0.43 mm wide, and the gaps between all electrodes are ~0.13 mm. The TW SLIM FF module consists of four sections: entrance, trap, funnel, and exit (Figure 1C). The FF entrance section was designed based on a configuration utilizing 6 rf strips interleaved by 5 arrays of TW electrodes (which we will subsequently refer to as 6,5) to transmit ions from the upstream regions (IFT) and transport them into the following FF trap section driven by the applied TW1 voltage. The trap section for ion accumulation is ~280 mm long and ~6 mm wide. Two sets of TW electrodes (Figure 1B) were used for ion filling and ejection: TW1 applied to the first set of TW electrodes to fill the trap region, and another set of TW electrodes interleaved with TW1 electrodes but using TW2 voltage that moves ions orthogonally to TW1 for ion ejection. A set of guard electrodes (guard1) (3 mm wide) was used to confine ions laterally in both the entrance and trap sections. At the interface of the trap and funnel sections, two gates (G1, G2) were employed and synchronized with the timing of TW1 and TW2 to control ion accumulation and ejection. The IFT conductance-limiting orifice (CL) was used to control the ion injection to the FF (Figure 1C). When ions are accumulating, TW1 is “on” while TW2 is “off” (all TW2 electrodes in the trap section grounded), G1 and G2 are turned on simultaneously (15 and 50 V to G1 and G2 electrodes, respectively) to block ions. For ion release TW1 is turned “off” (all TW1 electrodes in the trap section grounded), TW2 is switched “on”, the above G1 and G2 voltages are turned “off”, and TW3 voltages are applied to the G1 and G2 electrodes. The converging “funnel” configuration was designed to increasingly confine ions to a progressively narrower path as space charge effects are typically reduced due to the increasing IM separation of components. All TW and rf electrodes in the IM separation region are perpendicular to the electrodes in the accumulation region (Figure 1B). The ion exit region at the funnel “bottom” has the same 6,5 electrode arrangement as the entrance section and can be used for transmission of ions to the MS or to other TW SLIM modules for long path IM separations in the future. The TW3

voltage was used in the funnel and exit sections and could be independently optimized for IM resolution and ion transmission. A pair of guard electrodes (guard2) having a width of 3 mm extend along the sides of the funnel section as well as the exit section and provide lateral ion confinement. In the present design, the 6 rf strip electrodes used in entrance, trap, and exit sections are parallel to ion path (except at the corners where the rf strips are perpendicular to the ion path), as are the 260 rf strip electrodes used in the funnel section. Each funnel section strip extends to the guard2 electrodes, thus their length depends upon their position in the funnel (Figure 1B) with a 950 kHz rf waveform applied, 180° out-of-phase to adjacent rf electrodes. The TW voltages were applied to each subset of eight electrodes and repeated across each section. The sequence of dc voltages applied in this work involved simultaneous application of a potential to four sequential electrodes while the other four electrodes are maintained at ground potential. The dc voltage steps one electrode at a time to create the TW that propagates throughout each section in TW SLIM FF module.[36]

The pressure in TW SLIM FF module was measured using a convectron gauge (Granville-Phillips, Boulder, CO). Prior to ion introduction into the TOF MS pusher region, both continuous and pulsed ion currents could also be measured at the quadrupole positioned immediately following the conductance limit of the rear ion funnel (Figure 1A). Ion current pulses were amplified using a fast current inverting amplifier (model 428, Keithley Instrument, Inc., Cleveland, OH), and data was recorded using a TDS-784C digital oscilloscope (Tektronix, Richardson, TX).

Chemicals and Materials

Agilent low concentration ESI tuning mixture (Agilent, Santa Clara, CA) was directly infused for the optimization of the TW SLIM FF module. To estimate the trapped m/z range, a mixture was prepared using an equimolar 1 μM nine peptide mix (bradykinin acetate salt, kemptide acetate salt, angiotensin I human acetate salt hydrate, angiotensin II human, neurotensin, renin substrate tetradecapeptide porcine, substance P acetate salt hydrate, melittin from honey bee venom, and fibrinopeptide A human) (Sigma-Aldrich, St. Louis, MO), and Pierce LTQ ESI positive ion calibration solution (Thermo Fisher Scientific, Pittsburgh, PA).

RESULTS AND DISCUSSION

Conventionally, ion trap capacity is limited by both the confining pseudopotential fields as well as the trap volume, and typically constrained for practical reasons. For example, while the use of a long multipole for ion trapping is feasible, and trapping capacity would be expected to increase roughly in proportion with the length of the device, the benefits of a “narrow” pulse of ions for IM separations are significantly sacrificed by this approach. The IFT increased the trap size beyond that previously demonstrated, but ion populations are limited to ~6×10^6 charges if space charge effects leading to nonlinear accumulation and m/z bias are to be avoided.[22,24]

In this work we have exploited the flexibility of SLIM to explore a novel design allowing a greatly extended trapping region, and that minimized impacts of ion injection pulse width by

the use of an orthogonal ion extraction and IM separation region. Such a design is anticipated to serve as a first stage SLIM module for use in conjunction with long path SLIM IM modules.[38,39]

Characterization of Ion Injection and Accumulation in the TW SLIM FF Module

We gave significant attention to the optimization of performance by studying effects of the TW1 speed, TW1 amplitude, TW1 sequence, and guard 1 voltage in the entrance and trap sections during ion injection and filling. As the TW1 voltage was applied in the entire entrance section and interleaved with the TW2 voltage in the trapping section for ion filling, the TW1 as well as guard1 could potentially have a significant effect on the charge capacity of the TW SLIM FF module. Figure S-1A shows the number of charges measured at the quadrupole for low concentration Agilent tuning mix as a function of TW1 speed for a fill time of 486 ms, where each measurement was acquired by averaging 32 consecutive measurements. The results show that the maximum number of charges was obtained at the lower TW1 speed (20 m/s), decreased ~15% when TW1 speed was increased to 80 m/s, and then plateaued. For a TW1 amplitude of 10 V, the lower TW1 speeds resulted in ion “surfing” and serve to drive efficient filling of the trap section. The TW1 speed had little effect on the number of charges for a given fill time.

The effect of TW1 amplitude on the number of charges is shown in Figure S-1B. The number of charges at 7.5 V was significantly greater than that at 50 V at the same TW1 speed of 82 m/s. Ions cannot “fall” back into the preceding TW “micro trap” or “bin” at high TW1 amplitudes and are thus propelled to the end of the trapping section. When charge density during ion accumulation becomes excessive, complex phenomena can occur including ion biases and ion losses such as to electrode surfaces as well as the guard1 electrode (we briefly discuss such possibilities in the Supporting Information; see also Figure S-2). For the typically used guard1 voltage of 15 V, there was insufficient dc potential to confine ions laterally when the TW1 amplitude was increased to, e.g., 50 V. In the remainder of this work, a TW1 amplitude of 10 V was applied.

Different TW1 sequences were also explored, ranging from 10000000 to 11111111 (where 0 = 0 V, and 1 = an applied TW amplitude, 10 V, to the specified electrodes). The results in Figure S-1C indicate that the number of charges decreased only modestly from 1.95×10^8 using 10000000 to 1.75×10^8 using 11110000. Other TW1 sequences such as 10001000, 11001100, and 11101110 yielded similar signal intensities, indicating negligible or very minor effect of TW1 sequence on FF trapping performance. Additionally, at the optimized TW1 conditions, the guard1 bias was assessed based on the number of charges and evaluated in the range of 5–60 V, as shown in Figure S-1D. The number of charges increased as the guard1 voltages changed from 5 to 10 V and then decreased. Smaller numbers of charges obtained at extremely low guard1 bias such as 5 V can be attributed to inefficient lateral ion confinement and losses when space charge effects become significant. At high guard1 biases, for instance, 60 V, ion losses can alternatively be ascribed to effects due to rf heating as the ion cloud expands in the direction of the rf electrodes, or alternatively to insufficient rf confinement leading to loss of ions to electrode surfaces due to the increased effects of field penetration by the guard1 bias.[36]

The effects of the G2 voltage as well as rf potential applied to FF were also evaluated. The present TW SLIM FF module utilized a dual gate (G1 and G2) to block ions during ion accumulation. G1 was set to 15 V (equal to guard1 bias) for all experiments in this work, and the number of charges at specific fill and release times was measured at different G2 voltages. The measured number of charges remained approximately constant as G2 voltage varied from 10 to 80 V (Figure S-3A, Supporting Information). Thus, the dual gate provides robust ion blocking and the G2 voltage had a negligible effect on the trapping performance. As the charge density increases during ion accumulation, the role of the confining rf potential is increasingly important. An evaluation of the number of trapped charges was conducted for different rf amplitudes at 950 kHz (Figure S-3B, Supporting Information). An approximately linear increase of the accumulated charges was observed as rf amplitude increased from 220 V_{pp} to 340 V_{pp} (rf amplitude >360 V_{pp} caused electrical breakdown). Previous studies[34,36,37,39] have shown lower rf amplitudes (180–300 V_{pp}) to be sufficient for lossless ion transmission in SLIM modules, however, higher rf amplitudes (>300 V_{pp}) provide better ion confinement for trapping in the TW SLIM FF module under conditions of increased space charge effects.

Orthogonal Ion Ejection and Ion Mobility Separation in the FF

In the present design, TW2 was employed to orthogonally eject ions after an accumulation event and TW3 was applied to achieve IM separations. In this work the effects of TW2 speed, TW2 amplitude, and TW2 sequence on ions' release as well as TW3 speed, TW3 amplitude, TW3 Sequence, and guard 2 in the funnel and exit sections on ion transmission and ion mobility separation were explored and optimized. Initially, the TW2 speed was set to 82 m/s, while the TW2 amplitude and sequence were varied, as shown in Figure S-3C,D. The number of charges increased ~25% when TW2 amplitude increased from 5 to 25 V and then decreased ~10% as TW amplitude increased to 50 V from 35 V. The maximum number of charges was obtained in the range of 20–35 V. These observations indicate the TW2 amplitude and sequence have no significant effect on ion ejection (Figure S-3D). Further investigation into ion ejection efficiency is discussed in following sections.

Upon ejection, a large number of ions are released into the funnel section where TW3 is applied to transport them to the FF "bottom" and then to the MS. In this work, TW3 speed, amplitude and sequence as well as guard2 bias effects on ion transmission were evaluated. As shown in Figure S-4A,B, when ions are surfing (e.g., at a TW3 speed <40 m/s and an amplitude of 30 V, or TW3 speed of 82 m/s and amplitude >40 V), the number of charges is less than 6×10^7 demonstrating most ion losses are due to space charge effects. However, under the following conditions: TW3 speed >100 m/s at TW3 amplitude of 30 V or TW3 amplitude <30 V at TW3 speed of 82 m/s, the number of charges is maintained at ~1.7×10^8. Thus, the initial separation of the ion species assists in reducing the charge density (i.e., space charge effects) and improving ion transmission in the funnel and exit sections and should also be beneficial as a prelude to further separation in the future by coupling with a long serpentine path or multipass TW SLIM module.[39] Additionally, various TW3 sequences were characterized as well as guard2 bias (Figure S-4C,D). Reduced signal was found using TW3 sequences of 11111000–11111110, presumably due to overfilling of the smaller TW3 microtraps. The guard2 bias had no significant effect on number of charges

when larger than 15 V, consistent with previous studies.[34,36,37,39] The optimized conditions of all parameters for TW SLIM FF module are shown in Table S-1, Supporting Information.

Trapping Capacity and Efficiency

Ion currents for both continuous ion introduction from the IFT as well as in trapping modes for the TW SLIM FF module were directly measured (at the quadrupole in a differentially pumped region located after rear ion funnel). Comparisons of the observed ion currents provide insight into the trapping efficiency. Figure 2A shows the ion currents measured for the low concentration Agilent tuning mix acquired at different fill times in the TW SLIM FF module. These data show that IM separations were achieved in the FF. Peak intensities increased with fill time as more ions were accumulated, and both low and high m/z ion discrimination effects were also observed when the fill time was larger than 486 ms and ascribed to space charge effects. Figure 2A also shows that the maximum amplitude of the ion current pulse (3.0 nA at the fill time of 1782 ms) exceeds that of the continuous beam (120 pA) by more than 25-fold.

The number of charges released from the TW SLIM FF module was calculated from the areas under the traces in Figure 2A divided by the elementary charge (1.602×10^{-19} C) and is shown in Figure 2B. The number of charges increased as the fill time increases, and the charge capacity was 3.2×10^8. The linear range for quantitative utility for the TW SLIM FF module was at least 0.5×10^8 charges. This capacity exceeds by more than an order of magnitude the capacity of any ion trap we are aware of used with either IM or MS and represents a similar improvement over the corresponding charge capacity of the IFT.[24] The length of the trap section is 280 mm, implying a charge capacity of ~1.15×10^6 charges/mm.

The TW SLIM FF module greatly increases the maximum injected ion populations and a potential first stage to a long path SLIM IM module, ultimately enabling greater sensitivity in conjunction with much better resolution. The ion trapping efficiency (shown in Figure 2B as solid blue squares) was calculated as the ratio of the charge at the quadrupole rods after a single accumulation event to the charge delivered by the continuous beam over the same accumulation period (see Figure 2A). The trapping efficiency was ~80–90% for shorter fill times (<162 ms) and then decreased to 20–30% on approaching the charge capacity of the TW SLIM FF module (for accumulation times >1000 ms). The observed trapping efficiency at short fill times can be attributed to the imperfect ion transmission efficiency of ion optics between the injection quadrupole and the TW SLIM FF module and the decrease in trapping efficiency with extended fill times due to the increasing space charge.

Ion Ejection Efficiency

The ejection efficiency strongly depends on the TW2 speed. Figure S-5 shows the dependence of the number of charges on the release time at four TW2 speeds in the trap section (the fill time was fixed to 486 ms). A TW2 speed of 165 m/s (higher than TW3 speed in funnel section) led to poor ion ejection efficiency. Reduction of the TW2 speed from 165 to 41 m/s resulted in ~25% improvement in sensitivity at a release time of 1.62 ms. Fast ion release from the trap section is important for efficient coupling of the TW SLIM FF module to other TW SLIM modules, such as the 13-m long serpentine TW SLIM module recently

described,[39] and finally to the oa-TOF mass spectrometer. This indicates lower TW2 speed gives rise to more efficient ion ejection while higher TW2 speed results in lower ejection efficiency.

Figure 2C shows a comparison of the IM separations acquired using the TW SLIM FF module and the continuous ion current (i.e., signal obtained in continuous mode) for the low concentration Agilent tuning mix. These data illustrate that even for a short release time of 0.324 ms, the maximum signal intensity (1.0 nA) was much greater than the continuous ion current (120 pA). An increase in the release time resulted in a significant increase in the peak intensity. For instance, using a release time of 1.62 ms, the maximum signal intensity exceeded the continuous ion current by a factor of 13. Longer release times resulted in only a limited increase in the ion signal because the majority of analyte ions had already exited the trap section. An ideal ion trap device would allow for the rapid and effective release of ions regardless of ion gate release time. In practice, the ejection speed has an ion mobility dependence,[24] so that higher mobility ion species exit the trap section faster, and to some extent forcing a compromise between signal intensity, resolution, and possible mobility-based biases.

Ion Mobility Time-of-Flight Mass Spectrometry

Analyses similar to those using current detection were performed by combining the TW SLIM FF module with an Agilent 6224 TOF MS. As shown in Figure 3A, a wide m/z range from 200 to 2400 can be accumulated in the trap section and efficiently released and transmitted. The IM separation is similar to Figure 2A. The separation reduces space charge effects and constitutes a potential first step for coupling with other SLIM IM modules. Figure 3C shows some tailing for each peak. Since ions will occupy the entire 280 mm long trap section and are ideally expected to be trapped uniformly, the ions located in the middle of the trap section have a shorter path (390 mm) through the funnel compared to ions at the two ends of the trap section (414 mm). This likely contributes to the observed peak tailing. In addition, more subtle effects likely contribute involving space charge related phenomena; for example, where more ions are accumulated (e.g., m/z 622) there is more peak “tailing” observed than for less abundant ions (e.g., m/z 2122) (Figure S-6; Supporting Information) and which we tentatively attribute to space charge effects when ions are refocused at the end of the “funnel” section. We note, however, the tailing is limited and likely can be eliminated by use of an ion peak compression approach we have developed in future TW SLIM modules.[40]

We also compared performance (see Chemicals and Materials) for the TW SLIM FF module in continuous and trapping modes. The results (Figure 4A) indicate a similar range of ions (m/z 200–1500) observed in trapping and in continuous modes for the TW SLIM FF module. No significant ion discrimination was observed demonstrating TW SLIM FF module has wide m/z range for ion filling, trapping, ejection, and transmission. The present SLIM has not yet been optimized for low m/z ions (e.g., m/z 195); lower intensity was observed in the trapping mode in contrast to the continuous mode, indicating the rf, TW, dc parameters as well as the accumulation time needs to be optimized for improved low m/z ion transmission.

Chemical Noise Reduction

In addition to the increase in the number of transmitted ions to the TOF detector due to ion accumulation, more efficient desolvation of analyte ions due to the extended trapping time and potentially rf heating in the trap occurs. This results in removal of chemical background peaks attributed to the more complete desolvation of smaller ions in the TW SLIM FF module during ion trapping. Under conventional conditions, and in the absence of significant space charge effects, any heating due to the rf confinement is expected to be minimal but probably more important is the extended time for desolvation, as reported by and discussed previously related to a IFT study.[24] We speculate that the reduction in solvent charged cluster related signals contributes to the significant S/N ratio enhancement observed. Most of the solvent-related ions are in the lower m/z range, and a more pronounced background noise reduction might be evident here. Figure 4B shows detail for the m/z 440–520 range for both continuous and trapping modes. The background noise was ~10-fold lower in trapping mode and the S/N ratio was similarly enhanced by approximately an order of magnitude for lower abundance species. Finally, we note that if excessive space charge is avoided, it is obviously advantageous that any such “ion population evolution” occurs prior to ion ejection for IM separation, as it does naturally when an extended trapping event is utilized.

CONCLUSION

In this work, we have developed and characterized a TW SLIM ion trap module that enables interfacing to atmospheric pressure ionization sources, greatly increased ion trapping capacities, and improved ion utilization efficiency in conjunction with IM separations. All TW, rf, and dc voltage parameters in different sections of the SLIM FF for ion filling, trapping, ejection, and transmission have been systematically characterized for achieving higher ion utilization efficiency. Low TW1 speeds and amplitudes have been shown to be beneficial for efficient ion filling; TW1 waveform sequence, guard bias and the blocking voltages on dual gates have no significant effect on ion accumulating; TW2 amplitude and sequence have negligible influence on ion release while low TW2 speed gives faster ion ejection; high TW3 speed and low TW3 amplitude accompanied with large TW3 microtraps provide efficient ion transmission after ion release since the space charge effects are significantly reduced. A 25-fold increase in signal was observed based on comparisons of the pulsed ion current obtained from TW SLIM FF IM experiments compared to the use of a continuous ion current. The charge capacity (3.2×10^8 charges) was estimated to be more than an order of magnitude greater than the IFT. A broad m/z range of ions can be simultaneously trapped and reduced interfering chemical noise results, which can be largely attributed to the extended trapping times and more efficient desolvation of ions, as reported in a previous study.[24] We note that the relatively small imperfections in IM separations can be addressed by improved FF designs (e.g., correcting for the variation in IM path length) or after the ion funnel using an ion mobility peak compression approach to be described in a future publication, and that the present work suggests straight forward approaches for further increasing trapped ion populations.[40,41] Finally, we anticipate that the TW SLIM FF module can in the future be combined with long serpentine path SLIM or multipass SLIM modules to achieve high-sensitivity and high-resolution ion mobility separations.

Supplementary Material

Refer to Web version on PubMed Central for supplementary material.

Acknowledgments

Portions of this research were supported by grants from the National Institute of General Medical Sciences (Grant P41 GM103493), the Laboratory Directed Research and Development Program at Pacific Northwest National Laboratory, and the U.S. Department of Energy Office of Biological and Environmental Research Genome Sciences Program under the Pan-omics Program. This work was performed in the W. R. Wiley Environmental Molecular Sciences Laboratory (EMSL), a DOE national scientific user facility at the Pacific Northwest National Laboratory (PNNL). PNNL is operated by Battelle for the DOE under Contract DE-AC05-76RL0 1830.

References

1. Fenn JB, Mann M, Meng CK, Wong SF, Whitehouse CM. Science. 1989; 246(4926):64. [PubMed: 2675315]
2. Kanu AB, Dwivedi P, Tam M, Matz L, Hill HH. J. Mass Spectrom. 2008; 43(1):1. [PubMed: 18200615]
3. Paglia G, Astarita G, Yu K. LC GC Eur. 2015; 28(9):520.
4. Dwivedi P, Puzon G, Tam M, Langlais D, Jackson S, Kaplan K, Siems WF, Schultz AJ, Xun LY, Woodsd A, Hill HH. J. Mass Spectrom. 2010; 45(12):1383. [PubMed: 20967735]
5. Dwivedi P, Schultz AJ, Hill HH Jr. Int. J. Mass Spectrom. 2010; 298(1−3):78. [PubMed: 21113320]
6. Smolinska A, Hauschild AC, Fijten RRR, Dallinga JW, Baumbach J, van Schooten FJ. J. Breath Res. 2014; 8(2):027105. [PubMed: 24713999]
7. Li HL, Giles K, Bendiak B, Kaplan K, Siems WF, Hill HH. Anal. Chem. 2012; 84(7):3231. [PubMed: 22339760]
8. Baker ES, Burnum-Johnson KE, Ibrahim YM, Orton DJ, Monroe ME, Kelly RT, Moore RJ, Zhang X, Theberge R, Costello CE, Smith RD. Proteomics. 2015; 15(16):2766. [PubMed: 26046661]
9. McLean JA. J. Am. Soc. Mass Spectrom. 2009; 20(10):1775. [PubMed: 19646898]
10. Moon MH, Myung S, Plasencia M, Hilderbrand AE, Clemmer DE. J. Proteome Res. 2003; 2(6): 589. [PubMed: 14692452]
11. Valentine SJ, Kulchania M, Barnes CAS, Clemmer DE. Int. J. Mass Spectrom. 2001; 212(1−3):97.
12. Valentine SJ, Ewing MA, Dilger JM, Glover MS, Geromanos S, Hughes C, Clemmer DE. J. Proteome Res. 2011; 10(5):2318. [PubMed: 21417239]
13. Zhang X, Ibrahim YM, Chen TC, Kyle JE, Norheim RV, Monroe ME, Smith RD, Baker ES. Analyst. 2015; 140(20):6955. [PubMed: 26140287]
14. Midey AJ, Patel A, Moraff C, Krueger CA, Wu C. Talanta. 2013; 116:77. [PubMed: 24148376]
15. Valentine SJ, Kurulugama RT, Bohrer BC, Merenbloom SI, Sowell RA, Mechref Y, Clemmer DE. Int. J. Mass Spectrom. 2009; 283(1−3):149.
16. Kurulugama RT, Valentine SJ, Sowell RA, Clemmer DE. J. Proteomics. 2008; 71(3):318. [PubMed: 18590839]
17. Knorr FJ, Eatherton RL, Siems WF, Hill HH. Anal. Chem. 1985; 57(2):402. [PubMed: 3977072]
18. Dietiker R, di Lena F, Chen PJ. Am. Chem. Soc. 2007; 129(10):2796.
19. Clowers BH, Siems WF, Hill HH, Massick SM. Anal. Chem. 2006; 78(1):44. [PubMed: 16383309]
20. Szumlas AW, Ray SJ, Hieftje GM. Anal. Chem. 2006; 78(13):4474. [PubMed: 16808456]
21. Szumlas AW, Hieftje GM. Anal. Chim. Acta. 2006; 566(1):45.
22. Clowers BH, Ibrahim YM, Prior DC, Danielson WF, Belov ME, Smith RD. Anal. Chem. 2008; 80(3):612. [PubMed: 18166021]
23. Hoaglund CS, Valentine SJ, Clemmer DE. Anal. Chem. 1997; 69(20):4156.
24. Ibrahim Y, Belov ME, Tolmachev AV, Prior DC, Smith RD. Anal. Chem. 2007; 79(20):7845. [PubMed: 17850113]

25. Myung S, Lee YJ, Moon MH, Taraszka J, Sowell R, Koeniger S, Hilderbrand AE, Valentine SJ, Cherbas L, Cherbas P, Kaufmann TC, Miller DF, Mechref Y, Novotny MV, Ewing MA, Sporleder CR, Clemmer DE. Anal. Chem. 2003; 75(19):5137. [PubMed: 14708788]
26. Wyttenbach T, Kemper PR, Bowers MT. Int. J. Mass Spectrom. 2001; 212(1−3):13.
27. Pringle SD, Giles K, Wildgoose JL, Williams JP, Slade SE, Thalassinos K, Bateman RH, Bowers MT, Scrivens JH. Int. J. Mass Spectrom. 2007; 261(1):1.
28. Giles K, Williams JP, Campuzano I. Rapid Commun. Mass Spectrom. 2011; 25(11):1559. [PubMed: 21594930]
29. Tolmachev AV, Udseth HR, Smith RD. Anal. Chem. 2000; 72(5):970. [PubMed: 10739200]
30. Porobic T, Beck M, Breitenfeldt M, Couratin C, Finlay P, Knecht A, Fabian X, Friedag P, Flechard X, Lienard E, Ban G, Zakoucky D, Soti G, Van Gorp S, Weinheimer C, Wursten E, Severijns N. Nucl. Instrum. Methods Phys. Res., Sect. A. 2015; 785:153.
31. Grinfeld D, Giannakopulos AE, Kopaev I, Makarov A, Monastyrskiy M, Skoblin M. Eur. Mass Spectrom. 2014; 20(2):131.
32. Chen TC, Ibrahim YM, Webb IK, Garimella SVB, Zhang X, Hamid AM, Deng LL, Karnesky WE, Prost SA, Sandoval JA, Norheim RV, Anderson GA, Tolmachev AV, Baker ES, Smith RD. Anal. Chem. 2016; 88(3):1728. [PubMed: 26752262]
33. Zhang XY, Garimella SVB, Prost SA, Webb IK, Chen TC, Tang KQ, Tolmachev AV, Norheim RV, Baker ES, Anderson GA, Ibrahim YM, Smith RD. Anal. Chem. 2015; 87(12):6010. [PubMed: 25971536]
34. Webb IK, Garimella SVB, Tolmachev AV, Chen TC, Zhang XY, Norheim RV, Prost SA, LaMarche B, Anderson GA, Ibrahim YM, Smith RD. Anal. Chem. 2014; 86(18):9169. [PubMed: 25152066]
35. Webb IK, Garimella SVB, Tolmachev AV, Chen TC, Zhang XY, Cox JT, Norheim RV, Prost SA, LaMarche B, Anderson GA, Ibrahim YM, Smith RD. Anal. Chem. 2014; 86(19):9632. [PubMed: 25222548]
36. Hamid AM, Ibrahim YM, Garimella SVB, Webb IK, Deng LL, Chen TC, Anderson GA, Prost SA, Norheim RV, Tolmachev AV, Smith RD. Anal. Chem. 2015; 87(22):11301. [PubMed: 26510005]
37. Hamid AM, Garimella SVB, Deng L, Zheng X, Ibrahim YM, Webb IK, Anderson GA, Prost SA, Norheim RV, Tolmachev AV, Baker ES, Smith RD. Anal. Chem. 2016; 88(18):8949. [PubMed: 27479234]
38. Deng L, Ibrahim YM, Baker ES, Aly NA, Hamid AM, Zhang X, Zheng X, Garimella SVB, Webb IK, Prost SA, Sandoval JA, Norheim RV, Anderson GA, Tolmachev AV, Smith RD. Chemistry Select. 2016; 1(10):2396. [PubMed: 28936476]
39. Deng L, Ibrahim YM, Hamid AM, Garimella SVB, Webb IK, Zheng X, Prost SA, Sandoval JA, Norheim RV, Anderson GA, Tolmachev AV, Baker ES, Smith RD. Anal. Chem. 2016; 88(18): 8957. [PubMed: 27531027]
40. Garimella SVB, Hamid AM, Deng L, Ibrahim YM, Webb IK, Baker ES, Prost SA, Norheim RV, Anderson GA, Smith RD. Anal. Chem. 2016
41. Deng L, Garimella SVB, Hamid AM, Webb IK, Norheim RV, Prost SA, Zheng X, Sandoval JA, Baker ES, Ibrahim YM, Smith RD. 2016

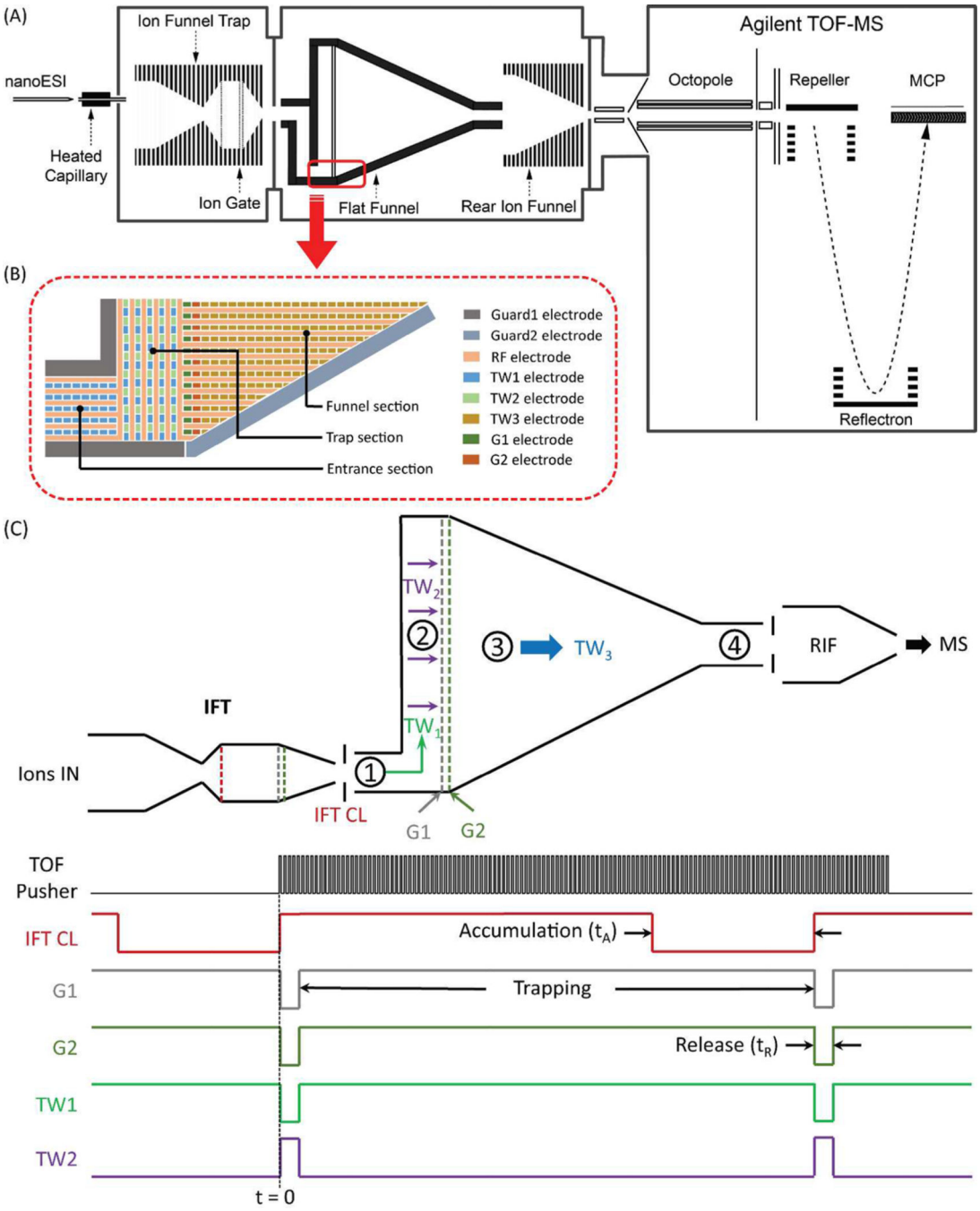

Figure 1.

(A) Representative schematic of the TW SLIM FF IM-MS instrument used in this work; (B) schematic of the TW SLIM FF intersection region showing the electrode arrangements of rf, TW, guard electrodes in different sections and dual gate (G1, G2) electrodes; (C) schematic diagram of TW SLIM FF (the numbers refer to the different sections (see text)) and IFT (it works in continuous mode and IFT CL is used to inject ions into TW SLIM FF as an entrance gate), and the pulse sequence and voltage profiles for ion accumulation and ejection. (All voltages were controlled using the same digital TTL signal. When it was high

(ion filling), IFT CL was open, G1 and G2 were close, TW1 was on and TW2 was off; while it was low (ion ejection), IFT CL was close, G1 and G2 were open, TW1 was off but TW2 was on).

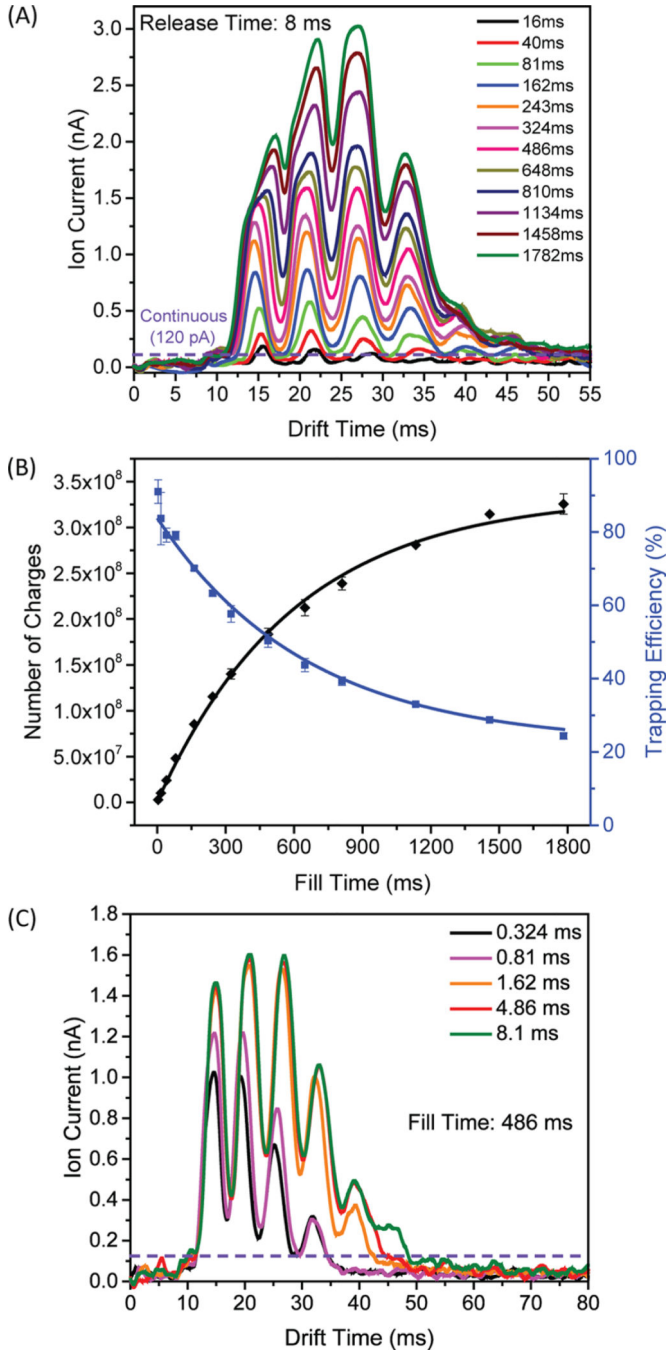

Figure 2.

(A) Ion current measurements at the quadrupole for ESI of the low concentration Agilent tuning mix solution with various fill times; (B) number of charges detected at the quadrupole as calculated from the areas under the above traces and the trapping efficiencies were calculated as a function of fill time; (C) ion current pulse measurements obtained at quadrupole with various release times. The following conditions were used: TW1 speed was 82 m/s, TW1 amplitude was 10 V, TW1 sequence was 11110000; TW2 speed was 82 m/s, TW2 amplitude was 30 V, TW2 sequence was 11110000; TW3 speed was 123 m/s, TW3

amplitude was 30 V, TW3 sequence was 11110000; Guard1 and guard 2 were set to 15 V; G1 was 15 V and G2 was 50 V; rf frequency was 950 kHz and rf amplitude was 320 V_{pp}; Gap was 3.15 mm and at 3.00 Torr pressure.

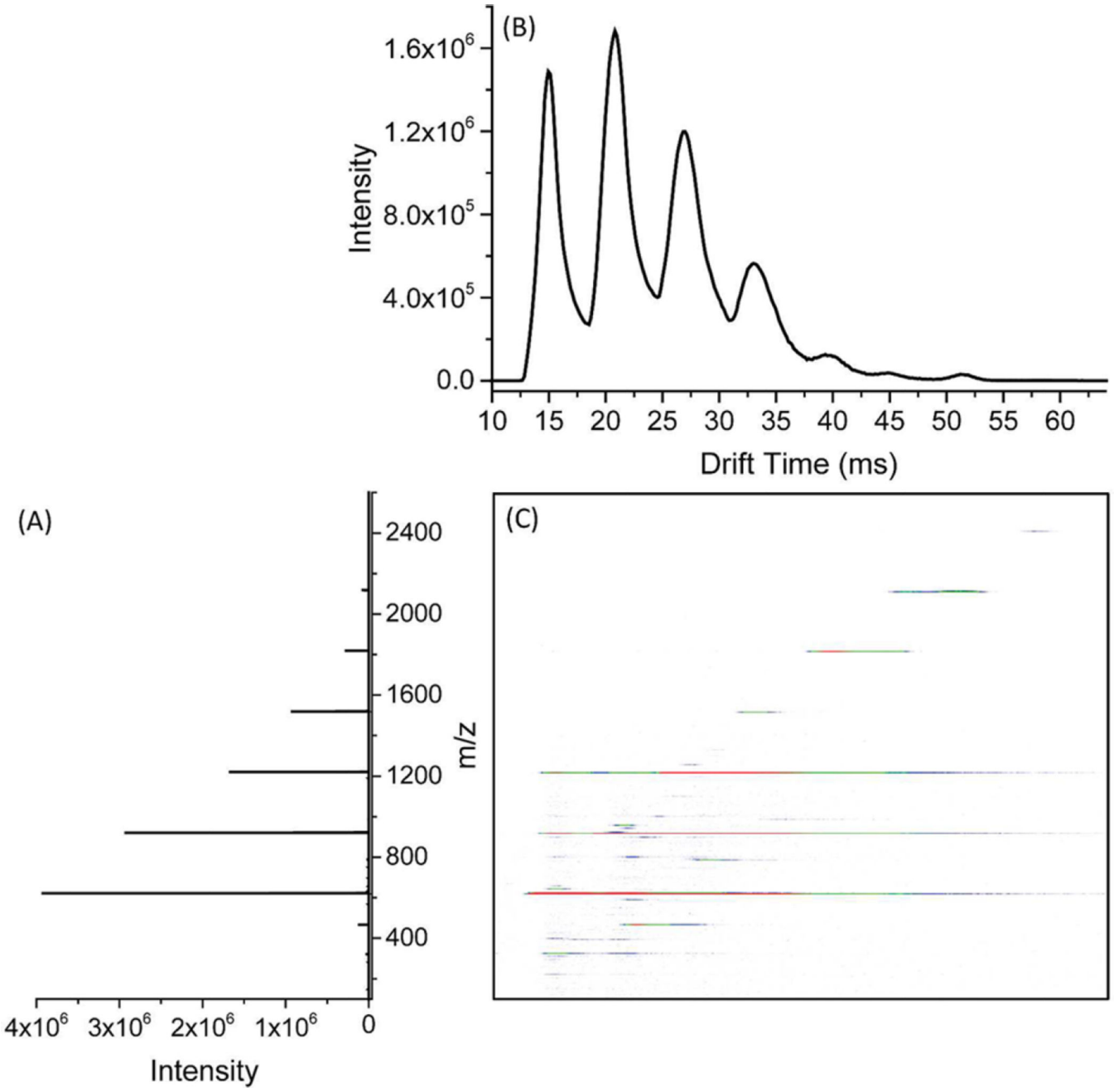

Figure 3.

(A) Mass spectrum of low concentration Agilent tuning mix obtained using the TW SLIM FF; (B) ion mobility spectrum was obtained by TW SLIM FF at the optimum conditions: TW1 speed was 82 m/s, TW1 amplitude was 10 V, TW1 sequence was 11110000; TW2 speed was 82 m/s, TW2 amplitude was 30 V, TW2 sequence was 11110000; TW3 speed was 123 m/s, TW3 amplitude was 30 V, TW3 sequence was 11110000; Guard1 and guard 2 were set to 15 V; G1 was 15 V and G2 was 50 V; rf frequency was 950 kHz and rf amplitude was 320 V_{pp}; fill time was 81 ms and release time was set to 1.62 ms; Gap was 3.15 mm and at 3.00 Torr pressure. (C) Nested mass and mobility spectrum.

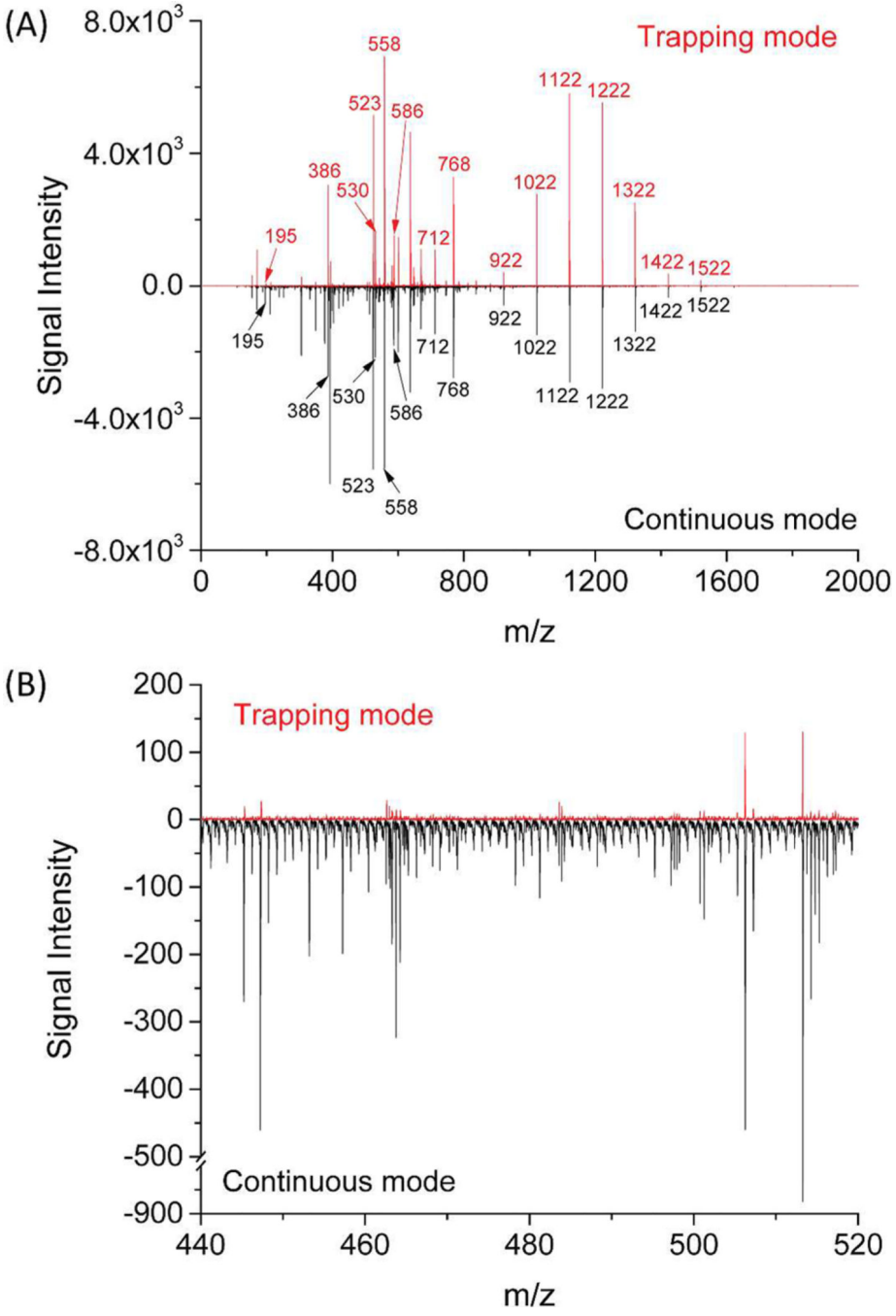

Figure 4.

(A) Mass spectra of nine peptides and ultramark mixture sample obtained using TW SLIM FF in the trapping and continuous modes. Other conditions of TW SLIM FF module were the same settings as Figure 3 at a release time of 8 ms in trapping mode and (B) zoomed in mass spectra in a narrow *m*/*z* range to show the significant noise reduction in trapping mode.